Solar Energy Materials and Solar Cells 201 (2019) 110060

Contents lists available at ScienceDirect

Solar Energy Materials and Solar Cells

journal homepage: www.elsevier.com/locate/solmat

Light-induced lifetime degradation effects at elevated temperature in Czochralski-grown silicon beyond boron-oxygen-related degradation

Michael Winter[a,b,*], Dominic Walter[a], Dennis Bredemeier[a,b], Jan Schmidt[a,b]

[a] Institute for Solar Energy Research Hamelin (ISFH), Am Ohrberg 1, 31860 Emmerthal, Germany
[b] Department of Solar Energy, Institute of Solid-State Physics, Leibniz University Hannover, Appelstr. 2, 30167 Hannover, Germany

ARTICLE INFO

Keywords:
LeTID
Czochralski-grown silicon
Boron-oxygen defect
Carrier lifetime

ABSTRACT

The effect of 'Light and elevated Temperature Induced Degradation' (LeTID) of the carrier lifetime is well known from multicrystalline silicon (mc-Si) wafers and solar cells. In this contribution, we perform a series of carrier lifetime measurements to examine, whether the same effect may also be observable in boron-doped Czochralski-grown silicon (Cz-Si). The Cz-Si samples of our study are illuminated (i) at room temperature, (ii) under standard regeneration conditions eliminating the boron-oxygen (BO) related defect (i.e. at 185 °C) and (iii) at a temperature of 80 °C, typical for the examination of the LeTID effect in mc-Si. We observe the typical decay of the carrier lifetime due to the activation of the BO-related defect. Beyond the BO degradation, applying standard solar cell processes, there is no indication for the activation of a second defect. On samples, whose surfaces are passivated by fired hydrogen-rich silicon nitride layers, an additional bulk lifetime degradation effect on a long timescale is observed in the Cz-Si material. However, defect generation rate and injection dependence of the lifetime suggest another defect type than the mc-Si-specific LeTID defect. We conclude that by applying processing steps that trigger LeTID in mc-Si, the same defect does not occur in the Cz-Si samples examined in this study. On a long timescale, however, a hitherto unknown type of defect is activated, which is different from the mc-Si-specific LeTID defect. A careful differentiation between the various kinds of recombination centres which may form during illumination at elevated temperatures is hence of utmost importance.

1. Introduction

The so-called 'Light and elevated Temperature Induced Degradation' (LeTID) effect [1–4] of the carrier lifetime in block-cast multicrystalline silicon (mc-Si) has become a steadily growing area of research over the last years. The firing step at the end of the solar cell production process was identified to trigger the degradation effect [4,5] and the firing peak temperature was shown to have a major impact on the extent of the lifetime degradation [6]. More recently, there have been publications indicating that a similar defect could exist in Cz-Si as well [7–9]. Other researchers, however, did not find any indications of the mc-Si-typical LeTID in Cz-Si material [10]. In addition, some publications reported LeTID in other types of monocrystalline silicon materials, such as Float-zone silicon and *n*-type Cz-Si [11–13]. In this study, we perform a series of experiments to clarify the apparent contradiction. We examine the carrier lifetime degradation under illumination of boron-doped Cz-Si material at increased temperatures to check, if the mc-Si-specific LeTID defect also occurs in Cz-Si material. We apply various process conditions to the Cz-Si wafers known to effectively trigger LeTID in mc-Si wafers.

2. Experimental details

We use standard boron-doped Cz-Si wafers with a base resistivity of 1.3 Ω cm. The saw damage of the wafers is removed in a KOH solution before cleaning them in a standard RCA sequence. The sample processing includes for most samples a phosphorus diffusion at 829 °C, resulting in n^+-diffused regions with a sheet resistance of either around 47 Ω/square or 100 Ω/square on both wafer surfaces. The phosphosilicate glass and the n^+-regions are in most cases removed afterwards using an HF-dip and a KOH solution, respectively. The wafer surfaces are passivated with an Al_2O_3/SiN_x-stack on both sides [14]. 10 nm of aluminum oxide (Al_2O_3) are deposited using plasma-assisted atomic layer deposition (Oxford Instruments, FlexAl). 100 nm of silicon nitride (SiN_x) with a refraction index of 2.05 (Meyer Burger, SiNA) or 120 nm with a refraction index of 2.4 (Oxford Instruments, Oxford Plasmalab 80 Plus), are deposited by plasma-enhanced chemical vapor deposition. Furthermore, on some wafers the Al_2O_3 layers are omitted. The wafers

* Corresponding author. Institute for Solar Energy Research Hamelin (ISFH), Am Ohrberg 1, 31860 Emmerthal, Germany.
E-mail address: m.winter@isfh.de (M. Winter).

https://doi.org/10.1016/j.solmat.2019.110060
Received 5 April 2019; Received in revised form 10 July 2019; Accepted 13 July 2019

receive a rapid thermal annealing (RTA) treatment corresponding to a typical firing step of screen-printed solar cells using an industrial conveyor belt furnace (centrotherm international, DO–FF–8.600–300). Two different measured peak temperatures (550 and 750 °C) with an uncertainty of ± 10 °C at a belt speed of 6.8 m/min are applied. Only the higher temperature of 750 °C is known to trigger the LeTID effect in mc-Si wafers, which was attributed to the in-diffusion of hydrogen from the silicon nitride and/or the dissolution of metal precipitates within the bulk [6]. The sample temperature is measured using a temperature tracker (Datapaq DQ1860A) and a type-K thermocouple (Omega, KMQXL-IM050G-300) within the furnace. The set peak temperatures were different for Cz-Si and mc-Si wafers to obtain the same actual peak temperatures due to the different surfaces textures of the two different material types. The set peak temperatures were 650 and 850 °C, respectively, for the Cz-Si wafers and 900 °C for the reference mc-Si wafers.

For our experiments, the wafers are cut into 5 × 5 cm^2 large samples after firing. The Cz-Si samples are annealed for 10 min at 200 °C in the dark to fully deactivate the BO defect. In order to investigate the impact of dark annealing on our reference mc-Si wafers [15], we compared the formation of the LeTID defect with and without previous dark annealing at 200 °C for 10 min. We observed no difference of the dark-annealed and the non-annealed mc-Si samples.

The Cz-Si samples are separated into three different groups to be exposed to different conditions. The standard test conditions are 80 °C and 1 sun (100 mW/cm^2) illuminated with a halogen lamp, i.e. typical LeTID defect activation conditions, as known from experiments on mc-Si samples [3,4]. Other samples are exposed to typical regeneration conditions (185 °C, 100 mW/cm^2) under which the BO defect is permanently deactivated [16]. Subsequently, the lifetime stability is examined at elevated temperature (80 °C, 100 mW/cm^2), i.e. under typical LeTID conditions. Cz-Si samples illuminated at room temperature (30 °C, 10 mW/cm^2) serve as a reference to characterize the BO defect activation. The lifetime is measured using a WCT-120 tester from Sinton Instruments and is analysed, if not stated otherwise, at a fixed excess carrier concentration of $\Delta n = 1 \times 10^{15}\,cm^{-3}$. Additionally, we investigate the injection dependence of the effective lifetime to distinguish between bulk- and surface-related effects and to extract the defect-specific hole-to-electron capture time ratio.

3. Experimental results and discussion

3.1. Lifetime degradation at 80 °C

Fig. 1 (a) shows the lifetime evolution for two Cz-Si samples fired at a measured peak temperatures of 750 °C (black circles) and 550 °C (blue triangles) and for an mc-Si sample fired at 750 °C as a reference (red squares). For the mc-Si sample (red squares), the typical LeTID behaviour is clearly visible. The fully degraded state is reached after approximately 100 h at 80 °C and 1 sun. The lifetime regeneration starts afterwards and lasts for another ~200 h. The Cz-Si sample fired at the same peak temperature, however, shows a completely different behaviour (black circles). The degraded state is reached in less than an hour at 80 °C and 1 sun which is fully attributed to the activation of the well-known BO defect [17], which is fully deactivated after another 20 h. The lifetime remains stable under prolonged illumination. The Cz-Si sample fired at a peak temperature of only 550 °C, which is not expected to show any LeTID, also shows a typical BO degradation/regeneration cycle (blue triangles in Fig. 1). Note that the rate constants of the deactivation process of the Cz-Si samples in Fig. 1 depend on the RTA peak temperature, which is well-known from the literature [16,18] and which is fully consistent with the faster regeneration at higher peak temperature observed in Fig. 1.

In Fig. 1 (b), the effective defect concentration N_d^* is shown for the same samples as shown in Fig. 1 (a). The defect concentration is defined as

$$N_d^*(t) = \frac{1}{\tau_d(t)} - \frac{1}{\tau_0}, \tag{1}$$

with the lifetimes of the degraded and initial (dark-annealed) states $\tau_d(t)$ and τ_0, respectively. The maximum effective defect concentration for the LeTID defect in the mc-Si sample is more than 4 times larger than the maximum concentration for the BO defect in the Cz-Si samples. Please note that the maximum defect concentration of the two Cz-Si samples fired at different peak temperatures is almost identical as is the defect generation rate which is expected, since the samples are processed from the same material.

To characterize the activated defects further, we determine the hole-to-electron capture time constant ratio Q via the linearized Shockley-Read-Hall (SRH) lifetime. Under the assumption of a deep level defect, the SRH lifetime it is given by Ref. [19].

$$\tau_{SRH} = \tau_{n0}\left(1 + Q\frac{n}{p}\right), \tag{2}$$

with the ratio of electron and hole concentrations n/p and the capture time constant ratio $Q = \tau_{p0}/\tau_{n0}$.

The obvious advantage of the SRH defect analysis in its linearized form is that a single defect manifests itself as a straight line. The capture ratio Q is determined at full degradation under the assumption of a single-level deep defect close to the middle of the band gap.

The SRH lifetime (which is the inverse of N_d^*) is normalised using the capture time constant τ_{n0} to display the capture ratio Q as the gradient of the linear fit. The normalised SRH lifetime is plotted in Fig. 2 versus n/p for the Cz-Si samples, which received an RTA at 750 and 550 °C peak temperature, respectively, and for the reference mc-Si sample fired at 750 °C. Since a second shallow defect is present in the

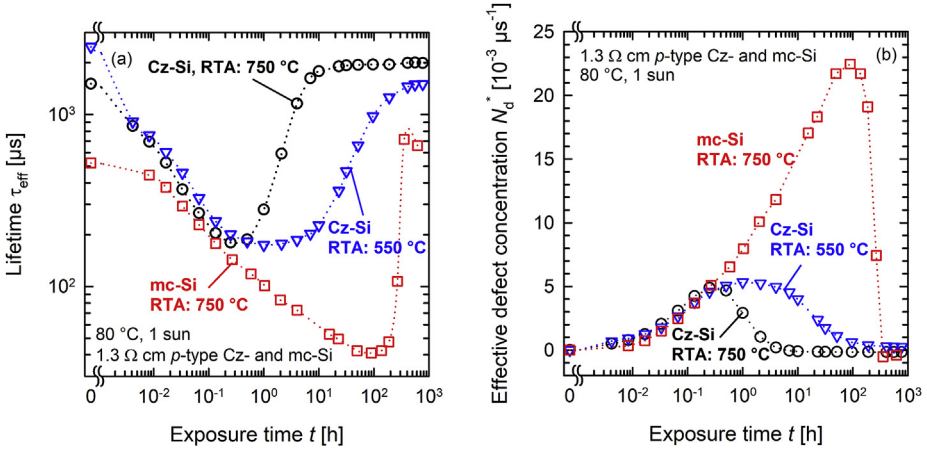

Fig. 1. (a) Effective lifetime τ_{eff} and (b) the corresponding effective defect concentration N_d^* versus the cumulative exposure time to 1 sun at 80 °C. Results are shown for two Cz-Si samples fired at the measured peak temperature of 750 °C (black circles) and 550 °C (blue triangles) and for a mc-Si sample of the same doping concentration as a reference (RTA: 750 °C, red squares). The dotted lines serves as guide to the eyes. (For interpretation of the references to colour in this figure legend, the reader is referred to the Web version of this article.)

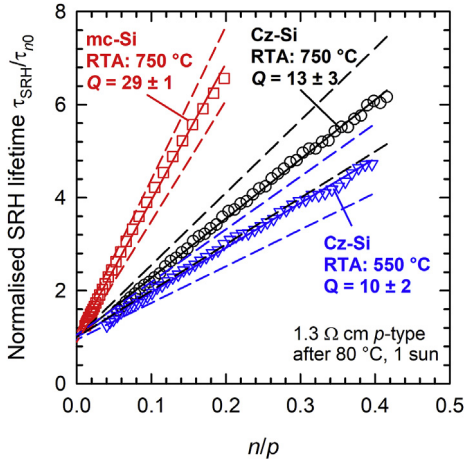

Fig. 2. Normalised SRH lifetime τ_{SRH}/τ_{n0} of the light-induced defect for two Cz-Si samples fired at different peak temperatures: 750 °C (black circles) and 550 °C (blue triangles) as a function of n/p. The solid lines are linear fits of Eq. (2) to the measured data and the dashed lines indicate the measurement uncertainty. The Q values extracted for the Cz-Si samples are characteristic for the BO defect. For comparison, the SRH lifetime for the LeTID defect of an mc-Si sample fired at 750 °C (red squares) is shown, resulting in a significantly higher Q value. (For interpretation of the references to colour in this figure legend, the reader is referred to the Web version of this article.)

mc-Si material, the analysis is only possible up to $n/p = 0.2$. The capture ratio Q for the LeTID-specific defect of the mc-Si sample is determined as $Q = 29 \pm 1$, which is in excellent agreement with the literature [20,21]. The Q value for the defect activated in the Cz-Si samples is $Q = 13 \pm 3$ for the higher and $Q = 10 \pm 2$ for the lower RTA temperature. Both values are in good agreement with the literature data of the BO defect, which is characterized by a Q value of ~10 [22,23]. The error margin is calculated with an assumed absolute error of the lifetime measurement of 10% (see dashed lines in Fig. 2).

3.2. Lifetime study at different temperatures

To examine the lifetime changes under our typical Cz-Si regeneration conditions (i.e. 185 °C, 1 sun) and to compare the maximum defect concentrations of samples degraded at temperatures close to room temperature (30 °C) and at 80 °C, a series of experiments is conducted at three different temperatures (185/80/30 °C) using identically processed Cz-Si samples. The results are shown in Fig. 3 (a). N_d^* is plotted versus the cumulative time the samples are exposed to the experimental conditions. The maximum effective defect concentration $N_{d,max}^*$ is considerably reduced for typical regeneration conditions of the BO-related defect (185 °C, 1 sun, black circles). After completed permanent deactivation of the BO defect (i.e., after about 10 min), the lifetime remains stable at a reduced temperature of 80 °C (for at least 800 h, which was the duration of our experiment.

In Fig. 3 (a), it is also visible that $N_{d,max}^*$ is almost identical for samples illuminated at 80 °C (blue inverse triangles) and at 30 °C (red squares). This is confirmed by Fig. 3 (b), which shows the injection-dependent lifetimes in the fully degraded state for both samples. The injection-dependent lifetimes are practically identical, which clearly supports that the same defect is limiting the lifetime in both samples. Additionally, the degraded lifetime for a sample fired at 550 °C (green triangles) is shown. Obviously, the same defect (namely the BO centre) is limiting the injection-dependent lifetime in samples treated at different RTA temperatures. The surface passivation, however, shows slight variations in quality, which is visible in the high-injection range of the samples shown in Fig. 3 (b). Although only the results of one Cz-Si material are presented here, the same experiments were also conducted for two other Cz-Si materials of comparable base resistivities, giving comparable results.

3.3. Impact of phosphorus diffusion

In order to examine a possible impact of the phosphorus diffusion, the P-diffusion was omitted for some samples. The results of a Cz-Si wafer with P-diffusion applied (black circles) and without (red squares) are shown in Fig. 4 (a). The lifetime in the fully degraded state is by a factor of 2 higher after the P-diffusion, which would be typically expected for the BO defect [24]. Aside from the BO defect activation and deactivation at 80 °C and 1 sun, no additional lifetime degradation effect is visible.

To approach the actual solar cell closer with our lifetime test structures, the n^+-diffused emitter region was left on the surface for some samples. The sheet resistance of the n^+-emitter was 100 Ω/square. The samples were exposed to typical BO regeneration conditions. After completed lifetime regeneration, the sample shown in Fig. 4 (b) is exposed to the elevated temperature of 80 °C at 1 sun, as indicated by the black vertical line. No substantial bulk lifetime degradation is occurring directly after regeneration. However, after ~40 h a degradation effect starts, which can be attributed to a degradation of the surface passivation quality. The saturation current density J_0, extracted around $\Delta n = 2 \times 10^{16}$ cm^{-3} using the Kane and Swanson method [25], increases over time from $J_0 = 40$ fA cm^{-2}(after 35 h) to $J_0 = 48$ fA cm^{-2} (after 1500 h).

3.4. Impact of the silicon nitride layer

It has been observed that the maximum concentration of the LeTID

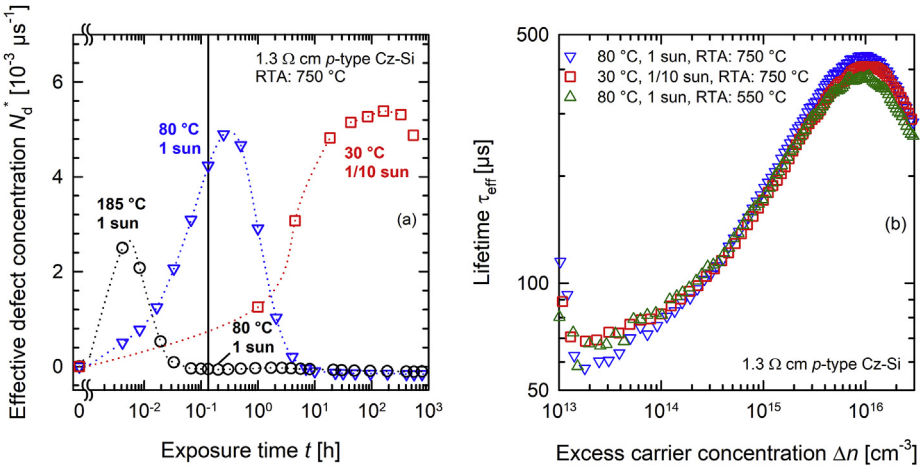

Fig. 3. (a) Effective defect concentration N_d^* for Cz-Si samples illuminated at different temperatures and intensities. While the dotted lines serve as guides to the eyes, the vertical line marks the change of temperature from 185 °C to 80 °C for the sample treated at 185 °C (black circles). (b) Injection dependent lifetimes in the fully degraded state for three different samples fired and illuminated at the specified temperatures and intensities.

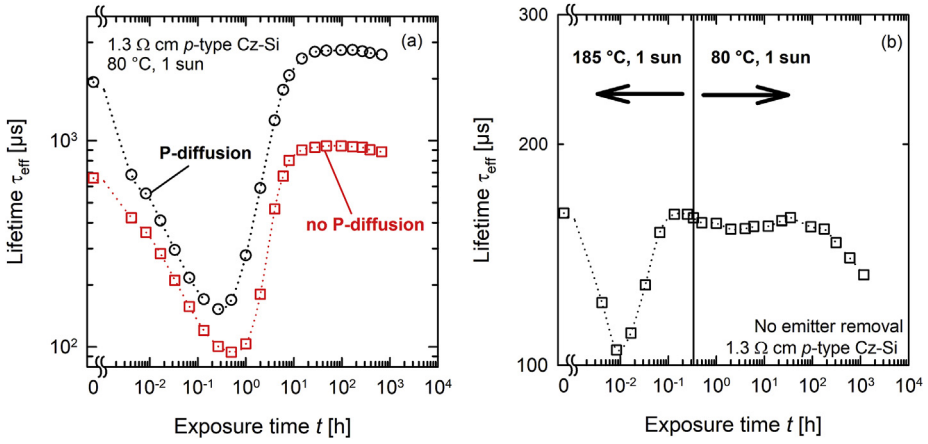

Fig. 4. (a) Effective lifetime τ_{eff} versus the cumulative exposure time to 1 sun at 80 °C of one Cz-Si sample each with (black circles) and without (red squares) applying a phosphorus diffusion during the processing. (b) Effective lifetime τ_{eff} for a sample whose n^+-emitter has not been removed during the processing. The vertical line marks the change of the experimental conditions from 185 °C to 80 °C at 1 sun. Dotted lines serve as guide to the eyes.

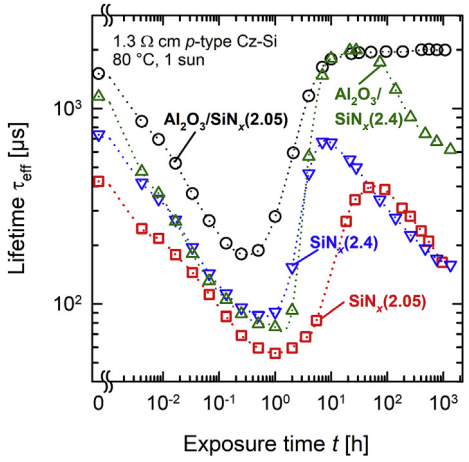

Fig. 5. Effective lifetime τ_{eff} versus the cumulative exposure time to 1 sun and 80 °C. Results are shown for four Cz-Si samples coated with different depicted dielectric layers and fired at the measured peak temperature of 750 °C. The values in brackets denote the refractive index (and hence the compositions) of the SiN_x layers applied.

defect in mc-Si changes with varying refractive index, and hence silicon content, of the hydrogen-rich SiN_x passivation layers, which was attributed to the increased in-diffusion of hydrogen into the silicon bulk. The maximum in-diffused hydrogen concentration was observed for silicon-rich SiN_x layers with a refractive index of 2.4 [26]. Hydrogen is hence considered to be one of the major contributors to the LeTID effect [11,13,26,27]. In order to examine, whether this effect can also be observed in Cz-Si, the dielectric layers used for surface passivation of the Cz-Si samples were varied. On the one hand, the refractive index (as measured by single-wavelength ellipsometry at $\lambda = 633$ nm) of the SiN_x is changed from the typical value of $n = 2.05$ to very silicon-rich SiN_x with $n = 2.4$. On the other hand, the underlying Al_2O_3 layer was omitted in some samples. The results are displayed in Fig. 5. The data recorded on the Cz-Si sample already discussed in subsection 3.1 (80 °C, 1 sun, Al_2O_3/SiN_x (2.05) stack, RTA: 750 °C) serve as a reference (black circles). The deactivation of the BO defect is completed after 45 h in the case of the single SiN_x layer with a refractive index of 2.05 (red squares), but already much faster after 10–20 h for the Al_2O_3/SiN_x (2.4) stacks (green triangles) and the silicon-rich SiN_x with a refractive index of 2.4 (blue inverse triangles). Interestingly, for these samples (in contrast to the reference sample shown as black circles in Fig. 5), we observe that after reaching the initial lifetime (or even a slightly higher lifetime value), the lifetime starts to degrade on the long term. This second degradation is still in progress for the samples after more than 1500 h at 80 °C and 1 sun.

An analysis of the capture ratio Q of the first formed defect centre (fully activated within 1 h at 80 °C and 1 sun) results in $Q = 16 \pm 5$ for the silicon-rich SiN_x ($n = 2.4$) and in $Q = 17 \pm 2$ for the Al_2O_3/SiN_x ($n = 2.4$) stack. These Q values are at the upper margin of the Q values reported in the literature for the BO defect [22,23], which could be an indication for the weak contribution by another defect with increased Q. Nevertheless, the BO activation is obviously dominant. For the $n = 2.05$ SiN_x single layers, the Q value is 12 ± 3, which is fully

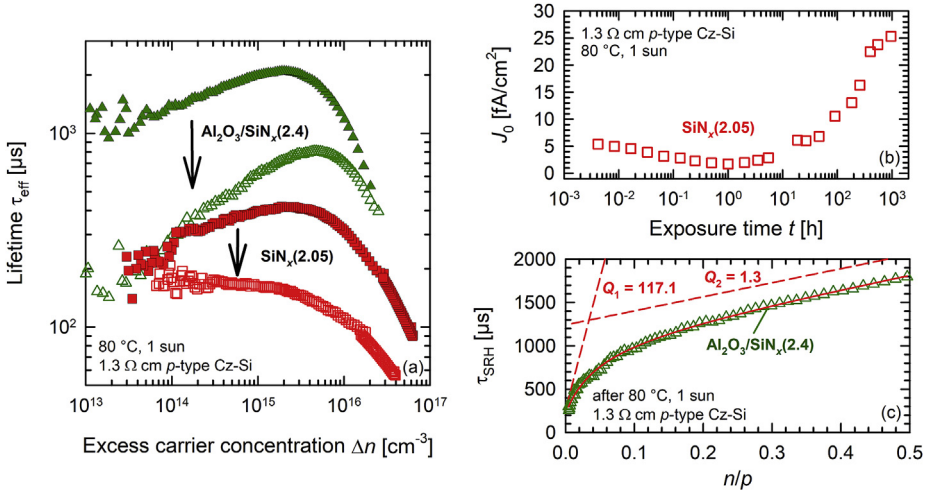

Fig. 6. (a) Injection-dependent lifetimes of two samples coated with Al_2O_3/SiN_x ($n = 2.4$) stack and SiN_x ($n = 2.05$), respectively. The regenerated lifetimes (closed green triangles and closed red squares) and the lifetime curves of the second degradation (open green triangles and open red squares) visible in Fig. 5 are shown. In the case of SiN_x (2.05), the injection dependent lifetime measurements are carried out using the photoconductance decay and quasi-steady-state photoconductance methods to broaden the accessible Δn range. (b) Saturation current density J_0 of the SiN_x (2.05)-sample plotted over the cumulative time the sample was exposed to 80 °C and 1 sun. J_0 was extracted around $\Delta n = 2 \times 10^{16}$ cm^{-3} following the Kane and Swanson [25] approach. (c) SRH lifetime τ_{SRH} of the second defect of the Al_2O_3/SiN_x (2.4)-sample after 1400 h of illumination as a function of n/p. (For interpretation of the references to colour in this figure legend, the reader is referred to the Web version of this article.)

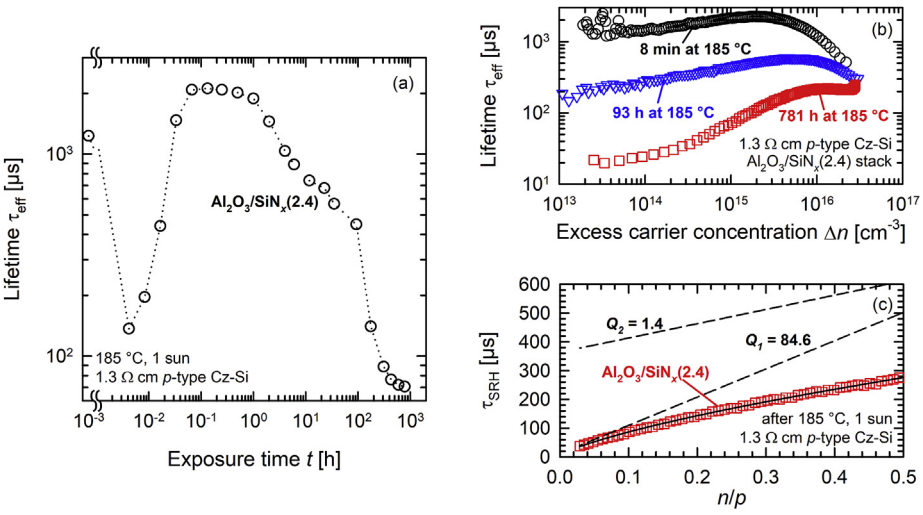

Fig. 7. (a) Effective lifetime τ_{eff} versus the cumulative exposure time to 1 sun and 185 °C of a sample coated with an Al_2O_3/SiN_x (n = 2.4) stack. The dotted line serves as guide to the eyes. (b) Injection dependent lifetime of the sample after 8 min (black circles), 93 h (blue inverse triangles) and 781 h (red squares) at 1 sun and 185 °C. (c) SRH lifetime τ_{SRH} of the second defect of the Al_2O_3/SiN_x (2.4) Cz-Si sample after 781 h at 1 sun and 185 °C as a function of n/p. (For interpretation of the references to colour in this figure legend, the reader is referred to the Web version of this article.)

consistent with the BO defect.

In Fig. 6, the regenerated lifetimes after the full deactivation of the BO defect (closed green triangles and closed red squares, after 20 and 45 h, respectively) and the lifetime of the second degradation effect (open green triangles and open red squares, after 1400 and 1000 h, respectively) are shown for the Al_2O_3/SiN_x (n = 2.4) stack and the single-layer SiN_x (n = 2.05) Cz-Si samples. Please note that the physical origins of the two observed degradation processes seems to be fundamentally different. Whereas the first relatively fast degradation visible in Fig. 5 is clearly a bulk-related effect with the activation of the BO complex being the dominant mechanism, a degradation of the surface passivation quality is largely responsible for the second degradation effect on the single-layer silicon nitride samples, as evidenced by the pronounced degradation at high injection densities (red squares in Fig. 6 (a)). As shown in Fig. 6 (b), the saturation current density J_0, extracted around $\Delta n = 2 \times 10^{16}$ cm^{-3} using the Kane and Swanson method [25], increases by a factor of 5 during the 1000 h of illumination. The degradation in the surface passivation is also observed for the silicon-rich SiN_x (n = 2.4) sample. However, the activation of a bulk defect covered by the degradation of the surface passivation quality cannot be ruled out.

Importantly, the Al_2O_3/SiN_x (n = 2.4) stack (green triangles in Fig. 6 (a)) shows a very different behaviour. The degradation is not visible in the high-injection regime, but at low injection levels and is therefore most likely caused by the activation of an additional bulk defect. However, the measured injection dependence is much weaker and therefore completely different from the one expected for the mc-Si-specific LeTID defect as well as of the BO defect. An analysis of the capture ratio Q plotted in Fig. 6 (c) reveals two defect states. Under the assumption of deep-level defects, the Q values can be determined to be $Q_1 = 117 \pm 60$ and $Q_2 = 1.3 \pm 0.5$. Please note that the square deviation was minimized to determine these Q values. Especially for Q_1, the determined value depends strongly on the selected injection range, which is the major reason for the large uncertainty. However, the Q value of the mc-Si-specific LeTID defect is ~30, which is well outside the range of Q_1 and Q_2.

In order to examine the formation of the new type of Cz-defect on a shorter timescale, Fig. 7 (a) shows the lifetime evolution of a Cz-Si sample coated with an Al_2O_3/SiN_x (n = 2.4) stack at 1 sun and 185 °C. The Cz-Si sample is processed identically to the one discussed in Figs. 5 and 6. In contrast to the mono-exponential long-term degradation observed in Fig. 5 (green triangles), the degradation visible in Fig. 7 (a) appears to be double-exponential. In Fig. 7 (b), the injection-dependent lifetime is depicted for the initial state of the long-term degradation (after 8 min at 185 °C and 1 sun, black circles), the intermediate state after 93 h (blue inverse triangles) and the fully degraded state after 781 h (red squares). The SRH defect analysis of the intermediate state (not shown here) reveals Q values in the same range as in Fig. 6 (c), that is $Q_1 = 83 \pm 40$ and $Q_2 = 1.5 \pm 0.5$. After complete degradation, we extract the same Q values, shown in Fig. 7 (c), of $Q_1 = 85 \pm 40$ and $Q_2 = 1.4 \pm 0.5$. Both recombination centres are most likely two different states of the same chemical defect of unknown composition.

4. Conclusion

In this contribution, we have performed a series of carrier lifetime experiments at different temperatures to trigger the mc-Si-specific LeTID defect in boron-doped Cz-Si. Most of our samples were coated with a typical Al_2O_3/SiN_x stack, where the SiN_x layer had a refractive index of n = 2.05. These samples were then fired in a conventional conveyor belt furnace. This firing is known to trigger the LeTID effect in mc-Si due to the in-diffusion of hydrogen from the hydrogen-rich SiN_x layer on the wafer surface into the silicon bulk. The hydrogen is currently believed to be one essential component causing LeTID in mc-Si. Although we provided optimal conditions for the formation of the LeTID defect, as shown on reference samples processed on mc-Si wafers, our experiments showed no indication of the activation of the mc-Si-specific LeTID defect in boron-doped Cz-Si. Nevertheless, in Cz-Si wafers coated with very silicon-rich SiN_x layers (n = 2.4), which are known to introduce a maximum amount of hydrogen into the silicon bulk, we in fact observed the formation of another new type of bulk defect on the long term. However, this defect showed very different recombination parameters compared to the LeTID defect, and can hence be considered as a different kind of (probably hydrogen-related) defect. For the application of typical SiN_x layers, no LeTID effect beyond the BO defect activation was observed in boron-doped Cz-Si in this study.

Acknowledgements

This work was funded by the German State of Lower Saxony and the German Federal Ministry of Economics and Energy within the research project LIMES (Contract no. 0324204D). The content is the responsibility of the authors.

References

[1] K. Ramspeck, S. Zimmermann, H. Nagel, A. Metz, Y. Gassenbauer, B. Birkmann, A. Seidl, Light induced degradation of rear passivated mc-Si solar cells, Proceedings of the 27th European Photovoltaic Solar Energy Conference and Exhibition, Frankfurt, Germany, 2012, pp. 861–865.

[2] K. Krauss, F. Fertig, D. Menzel, S. Rein, Light-induced degradation of silicon solar cells with aluminiumoxide passivated rear side, Energy Procedia 77 (2015) 599–606.

[3] F. Kersten, P. Engelhart, H.-C. Ploigt, A. Stekolnikov, T. Lindner, F. Stenzel, M. Bartzsch, A. Szpeth, K. Petter, J. Heitmann, J.W. Müller, Degradation of multicrystalline silicon solar cells and modules after illumination at elevated temperature, Sol. Energy Mater. Sol. Cells 142 (2015) 83–86.
[4] D. Bredemeier, D. Walter, S. Herlufsen, J. Schmidt, Lifetime degradation and regeneration in multicrystalline silicon under illumination at elevated temperature, AIP Adv. 6 (2016) 35119.
[5] K. Nakayashiki, J. Hofstetter, A.E. Morishige, T.-T.A. Li, D.B. Needleman, M.A. Jensen, T. Buonassisi, Engineering solutions and root-cause analysis for light-induced degradation in p-type multicrystalline silicon PERC modules, IEEE J. Photovoltaics 6 (2016) 860–868.
[6] D. Bredemeier, D.C. Walter, J. Schmidt, Lifetime degradation in multicrystalline silicon under illumination at elevated temperature: indications for the involvement of hydrogen, AIP Conference Proceedings, Lausanne, Switzerland, 2018, p. 130001.
[7] F. Fertig, R. Lantzsch, A. Mohr, M. Schaper, M. Bartzsch, D. Wissen, F. Kersten, A. Mette, S. Peters, A. Eidner, J. Cieslak, K. Duncker, M. Junghänel, E. Jarzembowski, M. Kauert, B. Faulwetter-Quandt, D. Meißner, B. Reiche, S. Geißler, S. Hörnlein, C. Klenke, L. Niebergall, A. Schönmann, A. Weihrauch, F. Stenzel, A. Hofmann, T. Rudolph, A. Schwabedissen, M. Gundermann, M. Fischer, J.W. Müller, D.J.W. Jeong, Mass production of p -type Cz silicon solar cells approaching average stable conversion efficiencies of 22 %, Energy Procedia 124 (2017) 338–345.
[8] D. Chen, M. Kim, B.V. Stefani, B.J. Hallam, M.D. Abbott, C.E. Chan, R. Chen, D.N.R. Payne, N. Nampalli, A. Ciesla, T.H. Fung, K. Kim, S.R. Wenham, Evidence of an identical firing-activated carrier-induced defect in monocrystalline and multicrystalline silicon, Sol. Energy Mater. Sol. Cells 172 (2017) 293–300.
[9] A. Graf, A. Herguth, G. Hahn, Determination of BO-LID and LeTID related activation energies in Cz-Si and FZ-Si using constant injection conditions, AIP Conference Proceedings, Leuven, Belgium, American Institute of Physics (AIP), 2019.
[10] H.C. Sio, H. Wang, Q. Wang, C. Sun, W. Chen, H. Jin, D. Macdonald, Light and elevated temperature induced degradation in p-type and n-type cast-grown multicrystalline and mono-like silicon, Sol. Energy Mater. Sol. Cells 182 (2018) 98–104.
[11] T. Niewelt, F. Schindler, W. Kwapil, R. Eberle, J. Schön, M.C. Schubert, Understanding the light-induced degradation at elevated temperatures: similarities between multicrystalline and floatzone p-type silicon, Prog. Photovolt. Res. Appl. (2017) 1–10.
[12] D. Sperber, A. Herguth, G. Hahn, A 3-state defect model for light-induced degradation in boron-doped float-zone silicon, Phys. Status Solidi RRL 11 (2017) 1600408.
[13] D. Chen, P.G. Hamer, M. Kim, T.H. Fung, G. Bourret-Sicotte, S. Liu, C.E. Chan, A. Ciesla, R. Chen, M.D. Abbott, B.J. Hallam, S.R. Wenham, Hydrogen induced degradation: a possible mechanism for light- and elevated temperature- induced degradation in n-type silicon, Sol. Energy Mater. Sol. Cells 185 (2018) 174–182.
[14] J. Schmidt, B. Veith, R. Brendel, Effective surface passivation of crystalline silicon using ultrathin Al2O3 films and Al2O3/SiNx stacks, Phys. Status Solidi RRL 3 (2009) 287–289.
[15] C. Chan, T.H. Fung, M. Abbott, D. Payne, A. Wenham, B. Hallam, R. Chen, S. Wenham, Modulation of carrier-induced defect kinetics in multi-crystalline silicon PERC cells through dark annealing, Sol. RRL 1 (2017) 1600028.
[16] D.C. Walter, B. Lim, K. Bothe, V.V. Voronkov, R. Falster, J. Schmidt, Effect of rapid thermal annealing on recombination centres in boron-doped Czochralski-grown silicon, Appl. Phys. Lett. 104 (2014) 42111.
[17] K. Bothe, J. Schmidt, Electronically activated boron-oxygen-related recombination centers in crystalline silicon, J. Appl. Phys. 99 (2006) 13701.
[18] S. Wilking, S. Ebert, A. Herguth, G. Hahn, Influence of short high temperature steps on the regeneration of boron-oxygen related defects, Proceedings of the 28th European Photovoltaic Solar Energy Conference and Exhibition, Paris, France, 2013, pp. 34–38.
[19] J.D. Murphy, K. Bothe, R. Krain, V.V. Voronkov, R.J. Falster, Parameterisation of injection-dependent lifetime measurements in semiconductors in terms of Shockley-Read-Hall statistics: an application to oxide precipitates in silicon, J. Appl. Phys. 111 (2012) 113709.
[20] A.E. Morishige, M.A. Jensen, D.B. Needleman, K. Nakayashiki, J. Hofstetter, T.-T.A. Li, T. Buonassisi, Lifetime spectroscopy investigation of light-induced degradation in p-type multicrystalline silicon PERC, IEEE J. Photovoltaics 6 (2016) 1466–1472.
[21] D. Bredemeier, D. Walter, S. Herlufsen, J. Schmidt, Understanding the light-induced lifetime degradation and regeneration in multicrystalline silicon, Energy Procedia 92 (2016) 773–778.
[22] J. Schmidt, A. Cuevas, Electronic properties of light-induced recombination centers in boron-doped Czochralski silicon, J. Appl. Phys. 86 (1999) 3175–3180.
[23] S. Rein, S.W. Glunz, Electronic properties of the metastable defect in boron-doped Czochralski silicon: unambiguous determination by advanced lifetime spectroscopy, Appl. Phys. Lett. 82 (2003) 1054–1056.
[24] K. Bothe, Oxygen-related Trapping and Recombination Centres in Boron-Doped Crystalline Silicon (Diss.), Leibniz University Hannover, 2006.
[25] D. Kane, R. Swanson, Measurement of the emitter saturation current by a contactless photoconductivity decay method, 18th IEEE Photovoltaic Specialists Conference, 1985, p. 578.
[26] D. Bredemeier, D.C. Walter, R. Heller, J. Schmidt, Impact of hydrogen-rich silicon nitride material properties on light-induced lifetime degradation in multicrystalline silicon, Phys. Status Solidi RRL 31 (2019) 1900201.
[27] M. Kim, D. Chen, M. Abbott, S. Wenham, B. Hallam, Role of hydrogen: formation and passivation of meta-stable defects due to hydrogen in silicon, AIP Conference Proceedings, Lausanne, Switzerland, 2018, p. 130010.